ENGINEERING AND BIOPHYSICAL ANALYSIS OF ALPHA ADRENERGIC RECEPTOR CRYSTALLOGRAPHY CONSTRUCTS

Zachary Leon Schools

A thesis submitted to the faculty at the University of North Carolina at Chapel Hill in partial fulfillment of the requirements for the degree of Master of Science in the Pharmacology Department in the School of Medicine.

Chapel Hill
2016

Approved by:

Bryan Roth

Lee Graves

Rob Nicholas

© 2016
Zachary Leon Schools
ALL RIGHTS RESERVED

ABSTRACT

Zachary Leon Schools: Engineering and biophysical analysis of alpha adrenergic receptor crystallography constructs
(Under the direction of Bryan Roth)

G protein-coupled receptors (GPCRs) are ubiquitously expressed membrane-spanning proteins that control all of human physiology. GPCRs are structurally complex and their mechanism of activation and signaling is not fully understood. Furthermore, there is a need for more subtype-selective and functionally selective drugs. Development of these drugs could be accelerated by obtaining crystal structures of GPCRs. One such family that could benefit from the structural information in a crystal structure is the Alpha Adrenergic receptors (ADRA). ADRA receptors control cardiovascular as well as peripheral and central nervous system functions, but lack subtype selective drugs. Thus, the ADRA receptor family was screened in parallel for thermostability and likelihood of crystal formation. ADRA1A-nBRIL bound to prazosin was found to be the best target for further crystallization efforts.

TABLE OF CONTENTS

CHAPTER 1: ENGINEERING ALPHA ADRENOCEPTOR CONSTRUCTS ……1

Introduction ……...…….….1

Methods …….....3

Results …….....5

Discussion ……...…7

References …….18

CHAPTER 1: ENGINEERING ALPHA ADRENOCEPTOR CONSTRUCTS

INTRODUCTION

G protein-coupled receptors (GPCRs) are membrane-spanning proteins that ubiquitously control human physiology. Generally, GPCRs consist of seven transmembrane helices and interconnecting extra- and intracellular domains. GPCRs have many ligands including amino acids, peptides, nucleotides, lipids, ions, neurotransmitters, exogenous small molecules, and light. When activated by these ligands, GPCRs allow cells to respond to extracellular stimuli by activating intracellular signal transducers. Many different signal transducers can couple to GPCRs, and thus GPCRs must be conformationally disordered enough to facilitate these interactions. Upon ligand binding, a subset of receptor conformations are stabilized[1]. The ensemble of conformations stabilized by a ligand will determine what transducers interact with the receptor, and furthermore what exact cell response will be elicited. This property of ligand-unique signaling is termed functional selectivity[2].

Functional selectivity augments the value of GPCRs as drug targets because signaling can be finely controlled. However, it is currently poorly understood. Uncovering the structural basis of functionally selective signaling would allow for the rational design of new drugs with mechanisms distinct from the current clinical pharmacotherapeutic toolkit. Up until recently drug development has focused on assaying canonical pathways that represent a narrow sliver of the information propagated by a GPCR in response to ligand binding. However, structural studies of GPCRs are difficult due to their intricate binding pockets. X-ray crystallography is a technique

that addresses this problem by offering atomic-level resolution of receptor conformation and ligand interaction. Additionally, GPCRs may have unifying structural mechanisms of activation that could be uncovered through attainment of a crystal structure[3].

In the past decade a wealth of GPCR crystal structures have been solved. This has established a workflow that can reliably express and purify large amounts of protein, as well as screen crystallization conditions in a high-throughput fashion[4-23]. This workflow relies on: genetic fusion of water-soluble proteins, an insect cell expression system, affinity chromatography purification, biophysical analysis, lipidic cubic phase crystallization, and X-ray diffraction. The goal of this workflow is to generate thermostable constructs of receptor protein and to reduce the infinite possible crystallization conditions using biophysical assays during the process.

Alpha adrenergic receptors (ADRA) are widely expressed in human tissues, including vasculature and the nervous system. ADRAs control smooth muscle contraction, vasoconstriction, as well as modulate cognitive functions such as arousal and working memory[24]. ADRAs also modulate the release of the endogenous agonists epinephrine and norepinephrine from the adrenal glands and nerve terminals. ADRA is separated into two families: α1 (ADRA1) and α2 (ADRA2). ADRA1 family receptors canonically couple to G_q transducers, activating Phospholipase C. ADRA2 family receptors canonically couple to $G_{i/o}$ transducers, which inhibits cellular production of cyclic AMP. Currently, drugs are available that select for either ADRA1 or ADRA2, but no drugs are available that can select for subtypes of these families: 1A, 1B, 1D, 2A, 2B, and 2C. Drugs targeting ADRAs treat hypertension, PTSD induced nightmares, and ADHD[25] among other diseases and disorders. Because of the lack of subtype selectivity in current ADRA1 and ADRA2 drugs, their mechanism of action is obscured. A crystal structure of

an ADRA family receptor could reveal differences in binding pockets that may lead to subtype-selective drugs, and thus better patient treatments and outcomes. Thus, crystallization of an ADRA was pursued in a parallel manner through generation of thermostable constructs and identification of the most thermostabilizing ligands.

METHODS

Cloning

Cloning methods followed standard established protocols. Wild-type receptor was amplified out of a Roth Lab TANGO construct[26]. Fusion proteins were then either inserted N-terminally or into ICL3 using multiplexed PCR reactions. For N-terminal fusion protein constructs, ICL3 was shortened using mutagenesis primers. Restriction sites Asc1 and Fse1 were added N-terminally and C-terminally respectfully to receptor-fusion protein constructs through primer overhang. The construct was then digested with Asc1 and Fse1 restriction enzymes (New England Biolabs) and ligated into an Asc1/Fse1 digested pFastBac (Thermo Fisher Scientific) vector. Ligated pFastBac constructs were then transformed into DH10Bac bacteria (Thermo Fisher Scientific) and positive clones were picked through blue/white lacZ selection. All primers used are shown in Table 1.

Expression

Baculoviral plasmids produced from DH10Bac transformations were transfected into *Spodoptera frugiperda* (Sf9) cells cultured in ESF 921 Cell Culture Medium (Expression Systems). These transfections were done in 12-well poly-D-lysine treated plates in volumes of 0.5 mL at a concentration of 1 million cells per mL using Cellfectin II (Thermo Fisher Scientific). After 5 day incubation, media was collected and cells removed by centrifugation. This media was used as “P0” stock for viral infection of Sf9 cells in larger volumes. Suspension cultures of 40 mL were then infected with P0 virus. After 3 day incubation, media was collected and cells removed by centrifugation. This media was used as “P1” stock for viral infection in volumes large enough for structural studies. An additional iteration of viral infection was used for some constructs to generate “P2” stocks if P1 stocks were not competent enough as

determined by viral titration. Virus stocks were titered using a CyAn ADP flow cytometer (Beckman Coulter) at 488 nm to excite an anti-gp64 antibody with a PE fluorophore[27].

Purification

Pelleted cells were lysed and homogenized in the presence of protease inhibitors (Roche Life Sciences). Membranes were then iteratively ultracentrifuged and homogenized in high-salt buffer conditions until membrane pellet supernatant showed <0.1 mg/mL protein. Membranes were then resuspended in 100 mM HEPES, 150 mM NaCl, 10 mM $MgCl_2$, 20 mM KCl at pH 7.5. Reactive cysteines were then alkylated by adding iodoacetamide to resuspended membranes. Receptor protein was then solubilized in 2% n-dodecyl-β-D-maltopyranoside (Anatrace), 0.2% cholesteryl hemisuccinate (Sigma-Aldrich). Following receptor solubilization membranes were centrifuged and supernatant collected.

Receptor protein was then purified from detergent using immobilized metal affinity chromatography (IMAC) with TALON Superflow Metal Affinity Resin (Clontech). Bound receptor was eluted from the IMAC column using 250 mM imidazole, then concentrated in Vivaspin 20 concentrators (GE Healthcare Life Sciences) and desalted in G-25 MiniTrap columns (GE Healthcare Life Sciences). His-tags were then removed by incubation with PreScission Protease (GenScript) overnight. Receptor was then flowed over IMAC resin again to remove proteins non-specifically binding to the resin. Receptor was then further concentrated in Vivaspin 500 concentrators (GE Healthcare Life Sciences).

Biophysical Assays

Analytical size-exclusion HPLC was used to assess purified receptor homogeneity. Receptor thermostability was measured by heating purified detergent-solubilized receptor in the presence of N-[4-(7-diethylamino-4-methyl-3-coumarinyl)phenyl]maleimide (CPM)[28]. Purified receptor was heated in 96-well plate wells using a thermocycler in 2° C increments. CPM fluorescence was read using a Mithras LB 940 (Berthold Technologies) with emission wavelength set to 463 nm after every temperature increment.

RESULTS

Construct generation

Wild-type ADRA protein was modified to reduce disorder and facilitate crystallization. The N- and C-terminal domains of each ADRA were truncated. Position of truncation for all six receptors was based on sequence alignment with previously solved GPCRs ranked by sequence homology to each receptor. Exact locations of truncation for each receptor are shown in Table 1. In addition to the terminal regions, the third intracellular loop (ICL3) was also truncated. ICL3 extensively interacts with signaling transducers, and is thus highly disordered and would likely inhibit crystallization. The strategy applied to terminal region truncation was also used for ICL3, and locations of these truncations are shown in Table 1.

Crystallization was further facilitated through genetic fusion of a water-soluble protein in the N-terminal or ICL3 regions. Fusion proteins assist in crystallization through improvement of receptor packing in the crystallization medium (source 48 from grant). These fusion proteins include T4 lysozyme (T4L), and cytochrome b_{562}RIL (BRIL); both have been used previously by many other groups to solve GPCR crystal structures. Constructs containing BRIL have N-terminal and ICL3 insertion locations. Constructs using T4L have an ICL3 insertion location.

Upon truncation of disordered regions and insertion of fusion proteins, receptor constructs were then shuttled into a pFastBac vector (Thermo Fisher Scientific) containing an N-terminal HA signal sequence as well as a C-terminal His-tag (HHHHHHHHHH) for purification of receptor by immobilized metal affinity chromatography.

Analytical size-exclusion chromatography

Receptor homogeneity increases likelihood of crystal formation, and thus purified receptor constructs were assayed for homogeneity by analytical size-exclusion chromatography (SEC) immediately after purification as well as after room temperature incubation for multiple days. Homogeneity was measured by observing the width of the receptor elution peak from the size-exclusion column. For each receptor construct, SEC was performed with different ligands to identify which would be used for crystallization. Figures 1-6 show ultraviolet absorption profiles during elution of purified receptor from the column. All receptors indicated refer to the N-terminal BRIL fusion constructs.

For ADRA1A, incubation with prazosin resulted in much higher protein yield as compared to other ligands or apoprotein (Figure 1). For this reason, ADRA1A ligand selection ceased here and prazosin was selected as the ADRA1A co-crystallization ligand. For ADRA1B ligands appeared equally stabilizing during the initial run (Figure 2), so purified protein was incubated at room temperature for one week before a SEC re-run. Incubation with prazosin was most effective at preventing accumulation of ADRA1B aggregate peaks, and thus it was selected as co-crystallization ligand. For ADRA1D (Figure 3), prazosin appeared to result in the most homogeneous peaks immediately after purification, but terguride prevented accumulation of aggregate during room temperature incubation.

ADRA2 family receptors showed smaller differences in homogeneity, which made it difficult to determine ideal co-crystallization ligands. ADRA2A initial SEC showed lisuride causing an earlier elution than all other ligands (Figure 4), however it was not attempted to reproduce this. Room temperature incubation did cause intended aggregation accumulation as indicated by the increased size in the earlier peaks, but no one ligand preserved homogeneity

more than others. Lisuride and MK912 prevented aggregation the most. ADRA2B showed similar results, indicating asenapine, rauwolscine, and lisuride as candidate ligands (Figure 5). ADRA2C ligands appeared identical after initial purification, but MK912, rauwolscine, and terguride preserved homogeneity the most after room temperature incubation (Figure 6).

Construct thermostability

Due to the inconclusive nature of the SEC results, an additional method of assaying ligand stabilization of receptor constructs was used. Purified receptor was incrementally heated in the presence of CPM, a compound that binds free sulfhydryl groups. As the receptor unfolds in increased temperatures, CPM binds free cysteines and becomes fluorescent[28]. In the present study, only ADRA2A and ADRA2B were assayed using this technique. Neither ADRA2A nor ADRA2B showed shifts in thermostability between ligands (Figure 7).

DISCUSSION

The goal of the present study was to produce ADRA constructs for crystallization, and determine ideal co-crystallization ligands to begin the pursuit of a solved crystal structure. Construct generation was a success. N-terminal and ICL3 BRIL constructs as well as ICL3 T4 lysozyme constructs have been cloned into a vector amenable to baculoviral plasmid production. Continuation of ADRA structural studies should be trivial. Figure 1 shows the current status of N-terminal BRIL constructs. ADRA1A is the most promising target, due to the higher yield seen when compared to other ligands incubating identical volumes.

However, constructs may still require extensive modification beyond their current status. Truncation positions of ICL3 may need to be shuffled, as well as N-terminal linker length.ADRA2 family constructs also still retain their entire intracellular helix, which may need

to be removed to improve crystal packing. Interestingly, ADRA1D differed in its preferred ligand from ADRA1A and ADRA1B. This may hint at some minor differences in the binding pocket that could be further revealed by a crystal structure.

Primer (Amino Acid Number)	Sequence
FWD CGAT + Asc1 + ADRA1A (A19)	CGATGGCGCGCCGGCTCCGGTGAACATTAGTAAG
REV ADRA1A (G349) + Fse1 + ATGC	ATGCGGCCGGCCGCCCTCCACTGCCTGGCTGGGGGGATG
FWD CGAT + Asc1 + ADRA1B (S35)	CGATGGCGCGCCGAGCACTCTGCCACAGTTGGATATCACG
REV ADRA1B (G369) + Fse1 + ATGC	ATGCGGCCGGCCTCCCCGGCATTGACAGCCCAGGATGCG
FWD CGAT + Asc1 + ADRA1D (A86)	CGATGGCGCGCCGGCCGTAGGCGGTCTGGTTGTGAG
REV ADRA1D (R422) + Fse1 + ATGC	ATGCGGCCGGCCCCTGCACTGACACCGAAGGAGTCTAAGG
FWD CGAT + Asc1 + ADRA2A (G15)	CGATGGCGCGCCGGGCACCGAAGCGCCCGGTGGAGGGGCTC
REV ADRA2A (V465) + Fse1 + ATGC	ATGCGGCCGGCCAACGATTCGTTTCCTATCGCCTCTGC
FWD CGAT + Asc1 + ADRA2B (D2)	CGATGGCGCGCCGGATCATCAGGATCCCTATTCTG
REV ADRA2B (W450) + Fse1 + ATGC	ATGCGGCCGGCCCCATGCAGTCTGGGTCCACGGCCTGC
FWD CGAT + Asc1 + ADRA2C (A33)	CGATGGCGCGCCGGCATCAGGCGCCTCATGGGGCCCTCC
REV ADRA2C (Q462) + Fse1 + ATGC	ATGCGGCCGGCCCTGTCGGAAGCCCCTTCGCCTGCGCC
FWD CGAT + Asc1 + nBRIL	CGATGGCGCGCCGGCTGATCTGGAAGACAATTG
FWD nBRIL + ADRA1A (A19)	ATTCAGAAGTACCTGGCTCCGGTGAACATTAGTAAG
FWD nBRIL + ADRA1B (S35)	ATTCAGAAGTACCTGAGCACTCTGCCACAGTT
FWD nBRIL + ADRA1D (A86)	ATTCAGAAGTACCTGGCCGTAGGCGGTCTG
FWD nBRIL + ADRA2A (R24)	TGCATACATTCAGAAGTACCTGCGGGCTACCCCATATTCTC
FWD nBRIL + ADRA2B (D2)	TGCATACATTCAGAAGTACCTGGATCATCAGGATCCCTATTCTG
FWD nBRIL + ADRA2C (G44)	TGCATACATTCAGAAGTACCTGGGCCAGTATAGCGCAGG
FWD ADRA1A ΔICL3 (D225 – T253)	AATCTGGGCTCAAGACCGATACCAAGACCCACTTTTCTGTCC
REV ADRA1A ΔICL3 (D225 – T253)	GGACAGAAAAGTGGGTCTTGGTATCGGTCTTGAGCCCAGATT
FWD ADRA1B ΔICL3 (E244 – R276)	GCCGGGGTCATGAAGGAGCGCAGTAGCATTGCCGTGAAGC
REV ADRA1B ΔICL3 (E244 – R276)	GCTTCACGGCAATGCTACTGCGCTCCTTCATGACCCCGGC
FWD ADRA1D ΔICL3 (R296 – S331)	GGCCGGCGTGAAACGGGAGCGCTCATCCCTGTCCGTAC
REV ADRA1D ΔICL3 (R296 – S331)	GTACGGACAGGGATGAGCGCTCCCGTTTCACGCCGGCC
FWD ADRA2A ΔICL3 (T246 – G364)	CCCCCCGGAGGCACAGGCAGACAAAACCGGGAAAAAAG
REV ADRA2A ΔICL3 (T246 – G364)	CTTTTTTCCCGGTTTTGTCTGCCTGTGCCTCCGGGGGG
FWD ADRA2B ΔICL3 (Q220 – A358)	AGGGGGAATCCAAGCAGGCACAGCTGACCAGAGAAAAG
REV ADRA2B ΔICL3 (Q220 – A358)	CTTTTCTCTGGTCAGCTGTGCCTGCTTGGATTCCCCCT
FWD ADRA2C ΔICL3(T260 – V372)	GCGCTTCCCCGACCACAGTCGCACAGGCGCGGG
REV ADRA2C ΔICL3(T260 – V372)	CCCGCGCCTGTGCGACTGTGGTCGGGGAAGCGC

Table 1. Complete list of all primers used in cloning of crystallization constructs, as well as truncation locations.

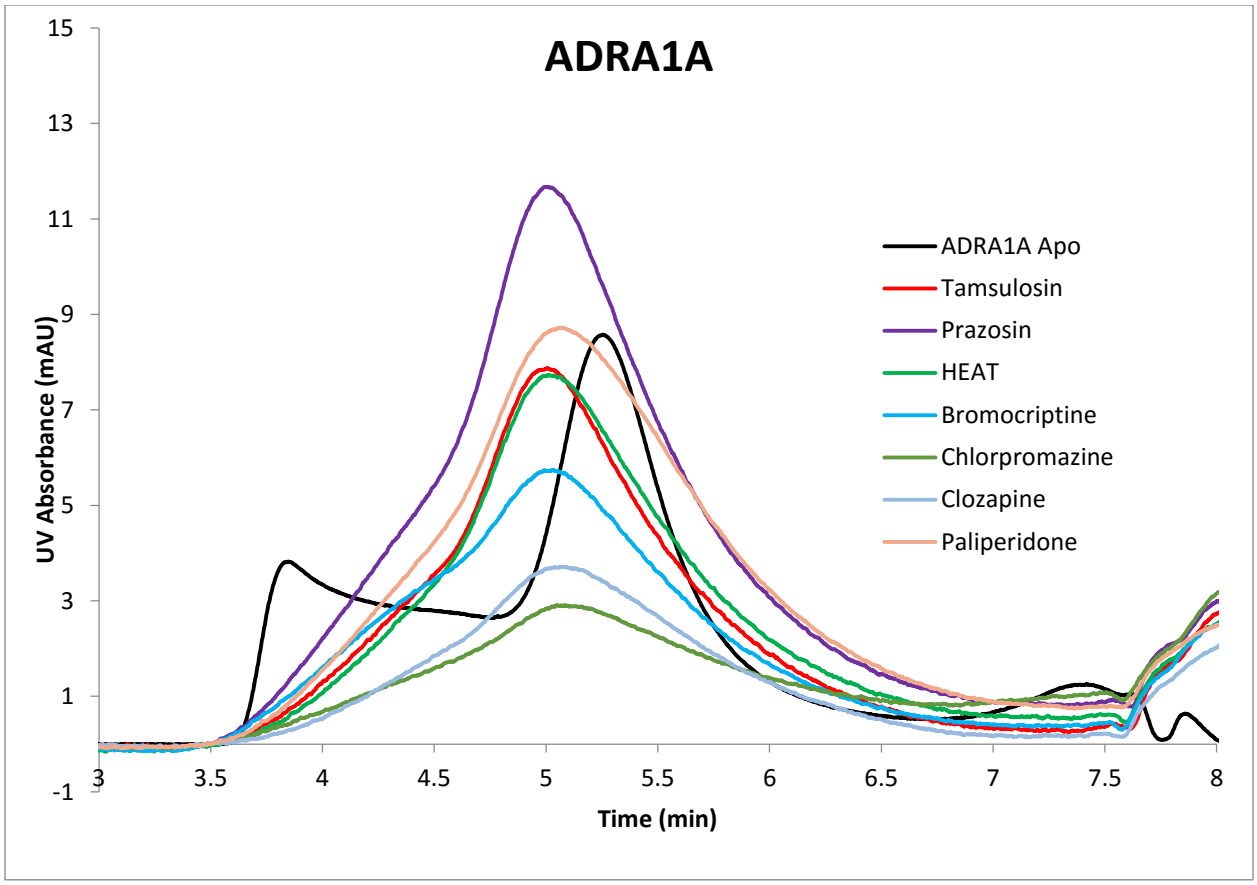

Figure 1. Ultraviolet absorbance in arbitrary units over time starting at Time = 0 when purified receptor was injected into the size-exclusion column by HPLC.

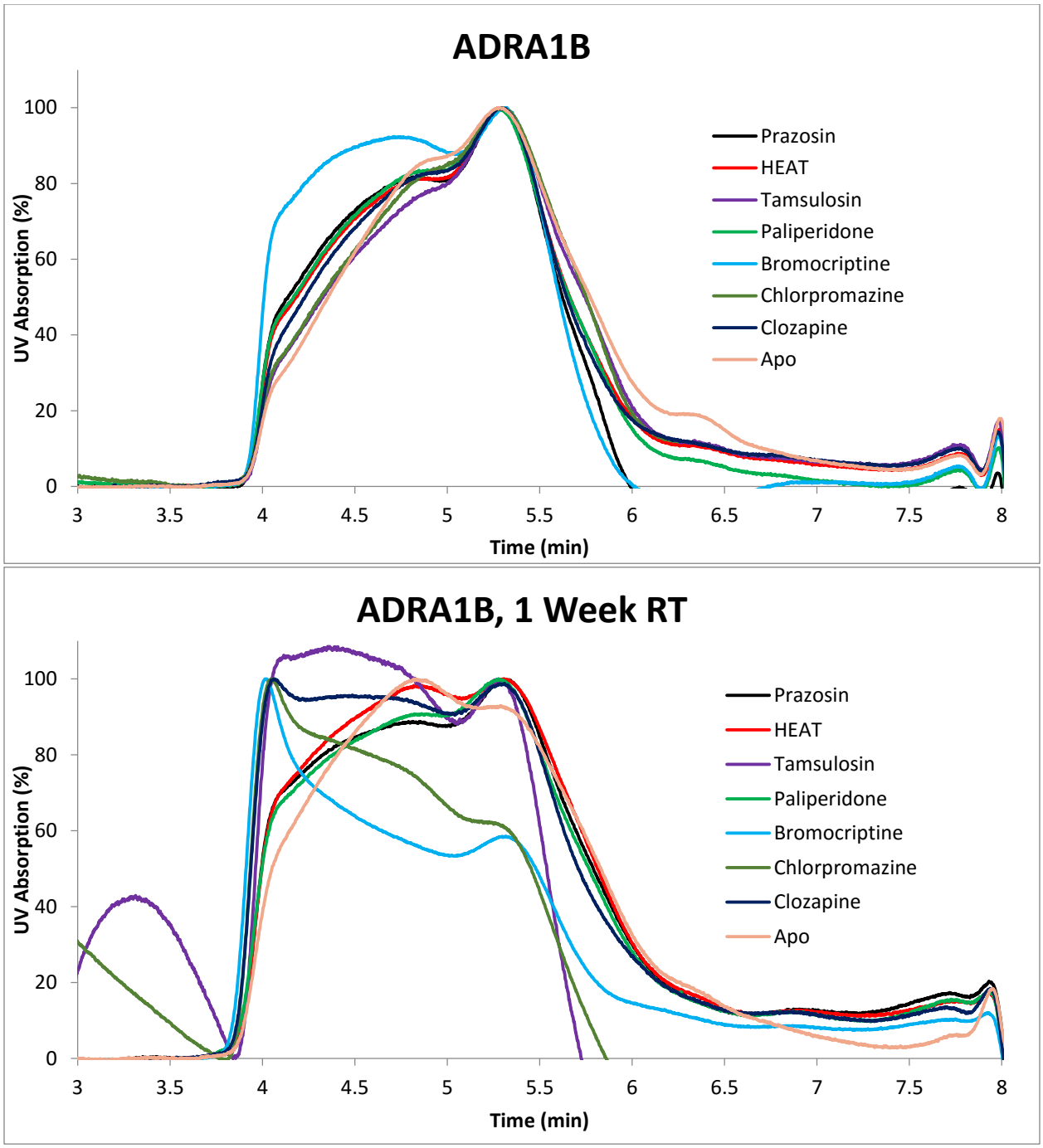

Figure 2. Ultraviolet absorbance in arbitrary units over time starting at Time = 0 when purified receptor was injected into the size-exclusion column by HPLC. Above, immediately after purification. Below, after one week incubation at room temperature.

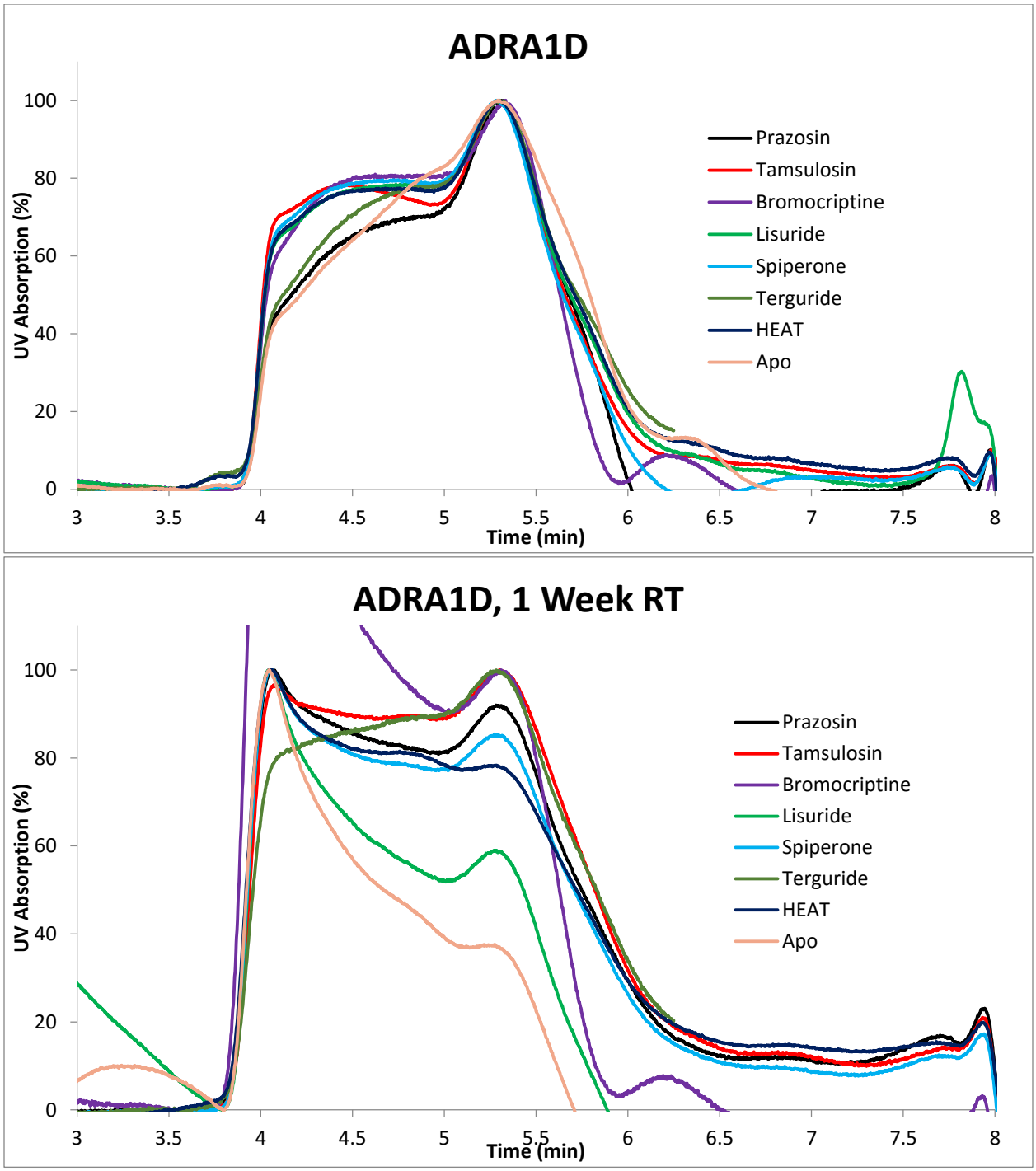

Figure 3. Ultraviolet absorbance in arbitrary units over time starting at Time = 0 when purified receptor was injected into the size-exclusion column by HPLC. Above, immediately after purification. Below, after one week incubation at room temperature.

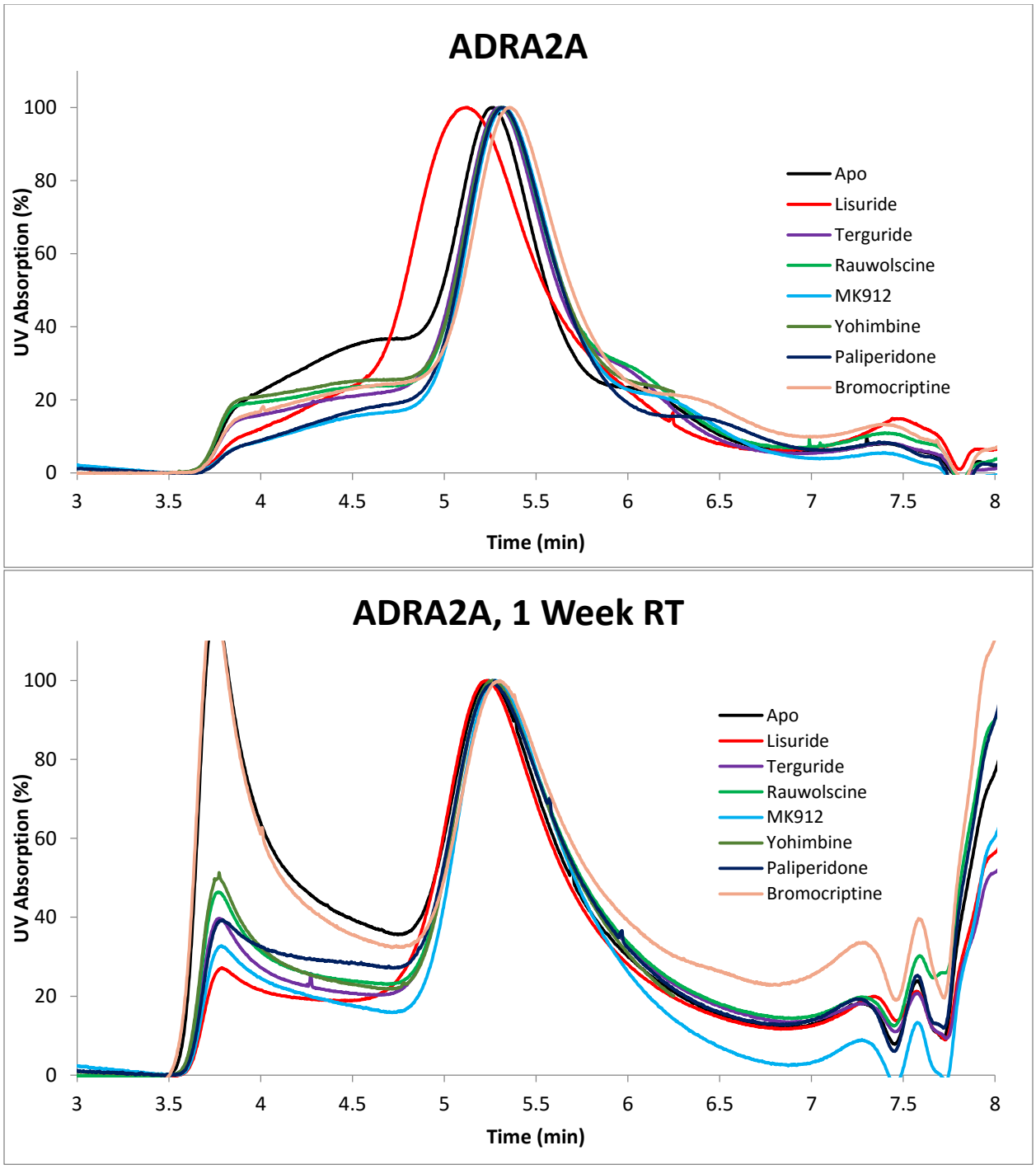

Figure 4. Ultraviolet absorbance in arbitrary units over time starting at Time = 0 when purified receptor was injected into the size-exclusion column by HPLC. Above, immediately after purification. Below, after one week incubation at room temperature.

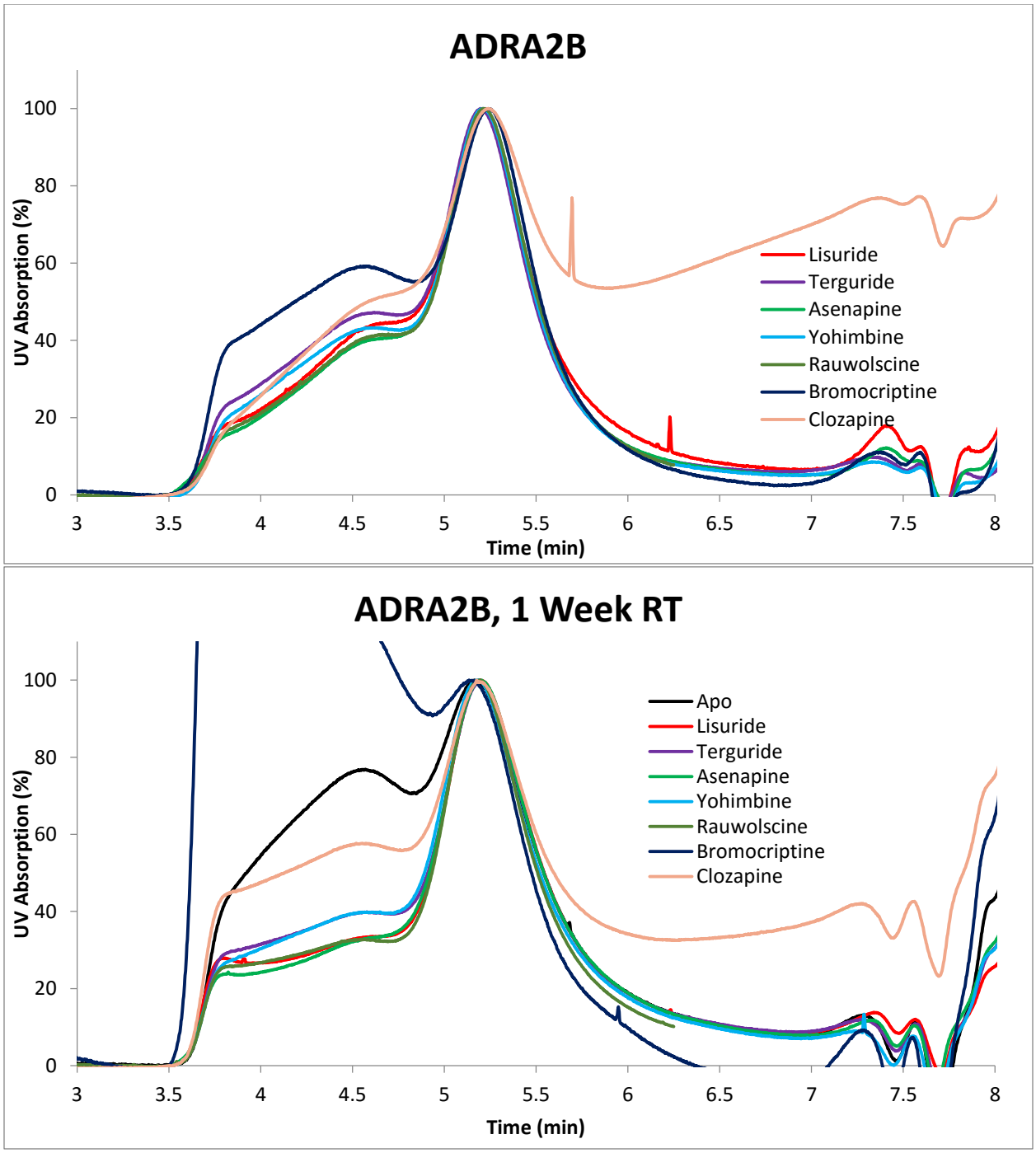

Figure 5. Ultraviolet absorbance in arbitrary units over time starting at Time = 0 when purified receptor was injected into the size-exclusion column by HPLC. Above, immediately after purification. Below, after one week incubation at room temperature.

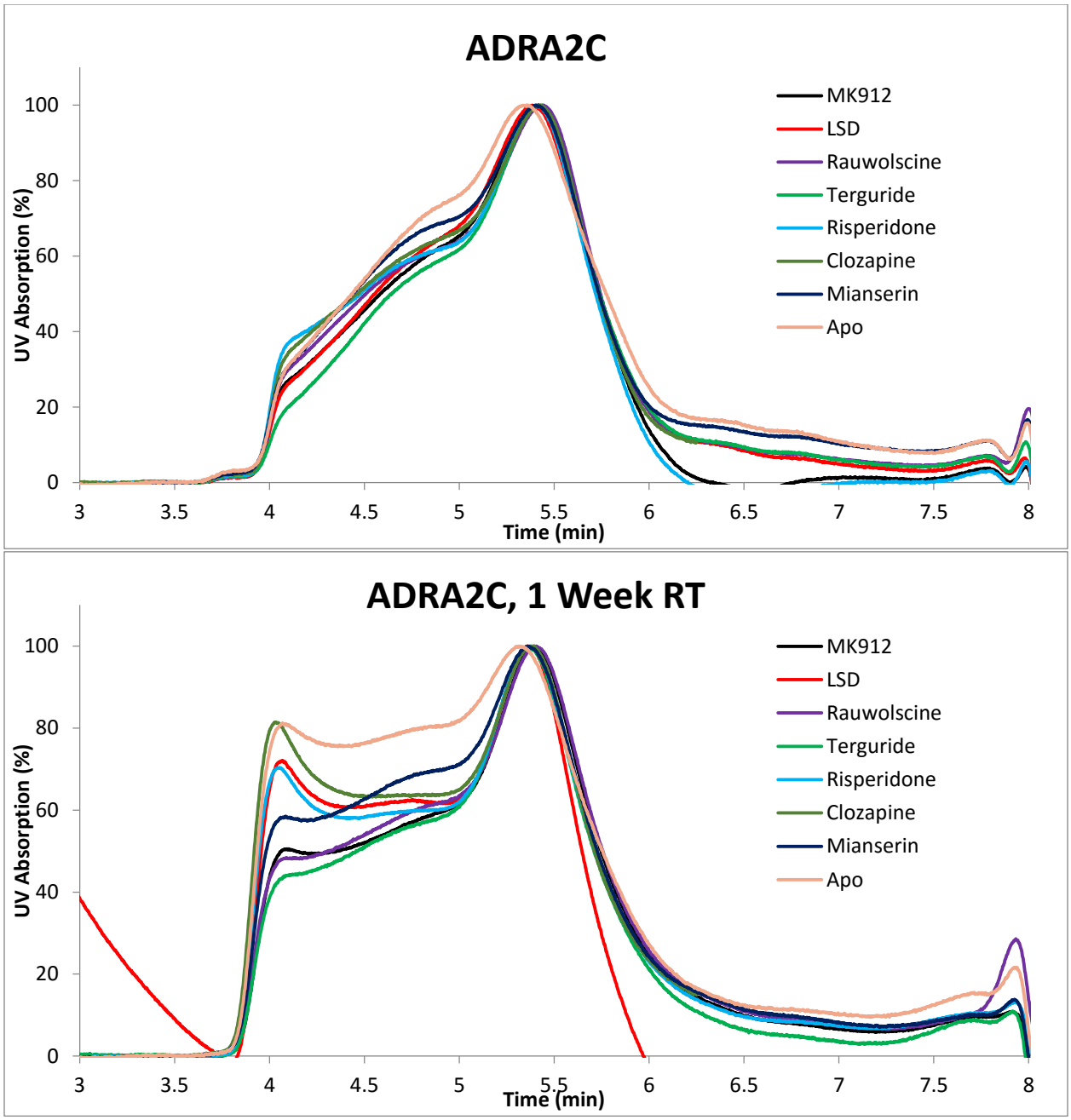

Figure 6. Ultraviolet absorbance in arbitrary units over time starting at Time = 0 when purified receptor was injected into the size-exclusion column by HPLC. Above, immediately after purification. Below, after one week incubation at room temperature.

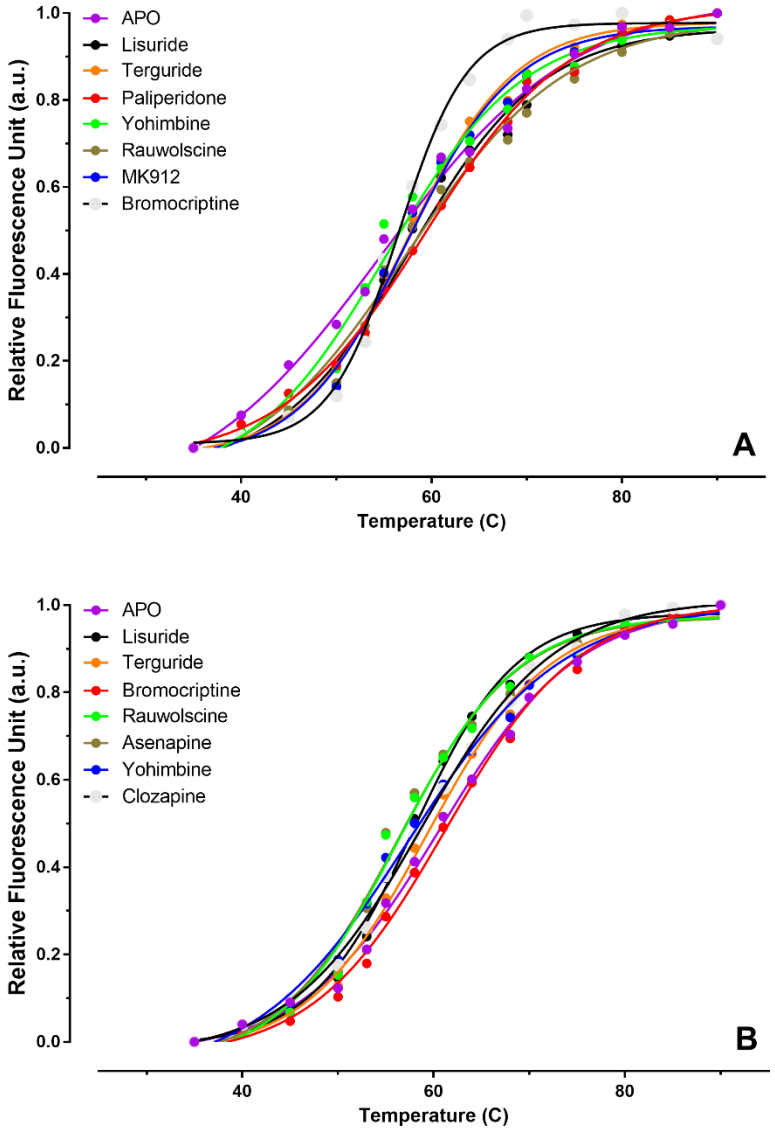

Figure 7. Melting curves for purified receptor obtained by heating purified receptor in the presence of CPM. A, ADRA2A-NBRIL. B, ADRA2B-NBRIL.

Receptor (n-BRIL)	Cloning	Ligand Screen	Thermostability	LCP Crystals
ADRA1A		Prazosin		
ADRA1B		Prazosin		
ADRA1D		Terguride		
ADRA2A		Inconclusive	Inconclusive	
ADRA2B		Inconclusive	Inconclusive	
ADRA2C		Inconclusive		

Table 2. Current progress of N-terminal BRIL ADRA constructs in the crystallization workflow.

REFERENCES

1. Motlagh HN, Wrabl JO, Li J, and Hilser VJ. (2014) The ensemble nature of allostery. *Nature* 508, 331-339

2. Urban JD, Clarke WP, Zastrow M, Nichols DE, Kobilka B, Weinstein H, Javitch JA, Roth BL, Christopoulos A, Sexton PM, Miller KJ, Spedding M, and Mailmain RB. (2007) Functional selectivity and classical concepts of quantitative pharmacology. *The Journal of Pharcology and Experimental Therapeutics* 320, 1-13

3. Tehan BG, Bortolato A, Blaney FE, Weir MP, Mason JS. (2014) Unifying family A GPCR theories of activation. *Pharmacology & Therapeutics* 143, 51-60

4. Wang C, Jiang Y, Ma J, Wu H, Wacker D, Han GW, Liu W, Huang XP, Vardy E, McCorvy JD, Gao X, Zhou XE, Melcher K, Zhang C, Bai F, Yang H, Yang L, Jiang H, Roth BL, Cherezov V, Stevens RC, and Xu HE. (2013) Structural basis for molecular recognition at serotonin receptors. *Science* 340, 610-614

5. Xu F, Wu H, Katritch V, Han GW, Jacobson KA, Gao ZG, Cherezov V, and Stevens RC. (2011) Structure of an agonist-bound human A2A adenosine receptor. *Science* 332, 322-327
6. Jaakola VP, Griffith MT, Hanson MA, Cherezov V, Chien YET, Lane JR, Ijzerman AP, and Stevens RC. (2008) The 2.6 Å crystal structure of a human A2A adenosine receptor bound to an antagonist. *Science* 322, 1211-1217

7. Liu W, Chun E, Thompson AA, Chubukov P, Xu F, Katritch V, Han GW, Roth CB, Heitman LH, Ijzerman AP, Cherezov V, and Stevens RC. (2012) Structural basis for allosteric regulation of GPCRs by sodium ions. *Science* 337, 232-236

8. Rosenbaum DM, Cherezov V, Hanson MA, Rasmussen SGF, Thian FS, Kobilka TS, Choi HJ, Yao XJ, Weis WI, Stevens RC, and Kobilka BK. (2007) GPCR engineering yields high-resolution structural insights into β2-adrenergic receptor function. *Science* 318, 1266-1273

9. Cherezov V, Rosenbaum DM, Hanson MA, Rasmussen SGF, Thian FS, Kobilka TS, Choi HJ, Kuhn P, Weis WI, Kobilka BK, and Stevens RC. (2007) High resolution crystal structure of an engineered human β2-adrenergic g protein-coupled receptor. *Science* 318, 1258-1265

10. Tan Q, Zhu Y, Li J, Chen Z, Han GW, Kufareva I, Li T, Ma L, Fenalti G, Li J, Zhang W, Xie X, Yang H, Jiang H, Cherezov V, Liu H, Stevens RC, Zhao Q, and Wu B. (2013) Structure of the CCR5 chemokine receptor – HIV entry inhibitor Maraviroc complex. *Science* 341, 1387-1390

11. Wu B, Chien EY, Mol CD, Fenalti G, Liu W, Katritch V, Abagyan R, Brooun A, Wells P, Bi FC, Hamel DJ, Kuhn P, Handel TM, Cherezov V, and Stevens RC. (2010) Structures of the CXCR4 chemokine GPCR with small-molecule and cyclic peptide antagonists. *Science* 330, 1066-1071

12. Chien Ey, Liu W, Katritch V, Han GW, Hanson MA, Shi L, Newman Ah, Javitch JA, Cherezov V, and Stevens RC. (2010) Structure of the human dopamine D3 receptor in complex with a D2/D3 selective antagonist. *Science* 330, 1091-1095

13. Fenalti G, Giguere PM, Katritch V, Huang XP, Thompson AA, Cherezov V, Roth BL, and Stevens RC. (2014) Molecular control of δ-opioid receptor signaling. *Nature* 506, 191-196

14. Siu FY, He M, de Graaf C, Han GW, Yang D, Zhang Z, Zhou C, Xu Q, Wacker D, Joseph JS, Liu W, Lau J, Cherezov V, Katritch V, Wang MW, and Stevens RC. (2013) Structure of the human glucagon class B g-protein-coupled receptor. *Nature* 499, 444-449

15. Srivastava A, Yano J, Hirozane Y, Kefala G, Gruswitz F, Snell G, Lane W, Ivetac A, Aertgeerts K, Nguyen J, Jennings A, and Okada K. (2014) High-resolution structure of the human GPR40 receptor bound to allosteric agonist TAK-875. *Nature* 513, 124-127

16. Shimamura T, Shiroishi M, Weyand S, Tsujimoto H, Winter G, Katritch V, Abagyan R, Cherezov V, Liu W, Han GW, Kobayashi T, Stevens RC, and Iwata S. (2011) Structure of the human histamine H1 receptor complex with doxepin. *Nature* 475, 65-70

17. Wu H, Wacker D, Mileni M, Katritch V, Han GW, Vardy E, Liu W, Thompson AA, Huang XP, Carroll FI, mascarella SW, Westkaemper RB, Mosier PD, Roth BL, Cherezov V, and Stevens RC. (2012) Structure of the human κ-opioid receptor in complex with JDTic. *Nature* 485, 327-332

18. Wu H, Wang C, Gregory KJ, Han GW, Cho HP, Xia Y, Niswender Cm, Katritch V, Meiler J, Cherezov V, conn PJ, and Stevens RC. (2014) Structure of a class C GPCR metabotropic glutamate receptor 1 bound to an allosteric modulator. *Science* 344, 58-64

19. Thompson AA, Liu W, Chun E, Katritch V, Wu H, Vardy E, Huang XP, Trapella C, Guerrini R, Calo G, Roth BL, Cherezov V, and Stevens RC. (2012) Structure of the nociceptin/orphanin FQ receptor in complex with a peptide mimetic. *Nature* 485, 395-399

20. White JF, Noinaj N, Shibata Y, Love J, Kloss B, Xu F, Gvozdenovic-Jeremic J, Shah P, Shiloach J, Tate CG, and Grisshammer R. (2012) Structure of the agonist-bound neurotensin receptor. *Nature* 490, 508-513

21. Zhang D, Gao ZG, Zhang K, Kiselev E, Crane S, Wang J, Paoletta S, Yi C, Ma L, Zhang W, Han GW, Liu H, Cherezov V, Katritch V, Jiang H, Stevens RC, Jacobson KA, Zhao Q, and Wu B. (2015) Two disparate ligand-binding sites in the human P2Y1 receptor. *Nature* 520, 317-321

22. Wang C, Wu H, Katritch V, Han GW, Huang XP, Liu W, Siu FY, Roth BL, Cherezov V, and Stevens RC. (2013) Structure of the human smoothened receptor bound to an antitumour agent. *Nature* 497, 338-43

23. Hanson MA, Roth CB, Jo E, Griffith MT, Scott FL, Reinhart G, Desale H, Clemons B, Cahalan SM, Schuerer SC, Sanna MG, Han GW, Kuhn P, Rosen H, and Stevens RC. (2012) Crystal structure of a lipid g protein-coupled receptor. *Science* 335, 851-855

24. Jakala P, Riekkinen M, Sirvio J, Koivisto E, Kejonen K, Vanhanen M, and Riekkinen P Jr. (1999) Guanfacine, but not clonidine, improves planning and working memory performance in humans. *Neuropsychopharmacology* 20, 460-470

25. Scahill L, Chappell PB, Kim YS, Schultz RT, Katsovich L, Shepherd E, Arnsten AF, Cohen DJ, and Leckman JF. (2001) A placebo-controlled study of guanfacine in the treatment of children with tic disorders and attention deficit hyperactivity disorder. *American Journal of Psychiatry* 158, 1067-1074

26. Kroeze WK, Sassano MF, Huang XP, Lansu K, McCorvy JD, Giguere PM, Sciaky N, Roth BL. (2015) PRESTO-Tango as an open-source resource for interrogation of the druggable human GPCRome. *Nature Structural & Molecular Biology* 22, 362-9

27. Li Z, Ling L, Liu X, Laus R, Delcayre A. (2010) A flow cytometry-based immuno-titration assay for rapid and accurate titer determination of modified vaccinia Ankara virus vectors. *Journal of Virological Methods* 169, 87-94

28. Alexandrov AI, Mileni M, Chien YET, Hanson MA, and Stevens RC. (2008) Microscale fluorescent thermal stability assay for membrane proteins. *Structure* 16, 351-359